Journal of Atmospheric and Solar–Terrestrial Physics 242 (2023) 105996

Contents lists available at ScienceDirect

Journal of Atmospheric and Solar-Terrestrial Physics

journal homepage: www.elsevier.com/locate/jastp

Research Paper

Winter surface air temperature variation over Pakistan during 1970–2014 and its principal drivers in the tropical ocean

Rizwan Karim [a,b,c], Guirong Tan [b,c,*], Brian Ayugi [d], Mohamed Abdallah Ahmed Alriah [e], Hamida Ngoma [f]

[a] Scientific Research Center of Xishuangbanna Tropical Botanical Garden, University of Chinese Academy of Sciences, Menglun Town, Mengla County, Xishuangbanna Prefecture, Yunnan, PR China
[b] Key Laboratory of Meteorological Disaster, Ministry of Education (KLME)/Joint International Research Laboratory of Climate and Environment Change (ILCEC), Nanjing, University of Information Science and Technology, Nanjing, 210044, China
[c] Collaborative Innovation Center on Forecast and Evaluation of Meteorological Disasters (CIC-FEMD), Nanjing, University of Information Science and Technology, Nanjing, 210044, China
[d] Department of Civil Engineering, Seoul National University of Science and Technology, 01811, Seoul, Republic of Korea
[e] School of Geographical Sciences, Nanjing University of Information Science and Technology, Nanjing, 210044, China
[f] Department of Geosciences, University of Connecticut, Storrs City, Connecticut, 06269, USA

ARTICLE INFO

Keywords:
DJF month'S temperature events (DJFTs)
Dipole mode index-eastern (DMIE)
Empirical orthogonal function (EOF)
Composite analysis
Advection

ABSTRACT

This study examined the leading modes of Dec–Feb (DJF) month's surface temperature (DJFTs) and associated mechanisms of the most significant drivers affecting temperature variability during the season from 1970 to 2014. EOF1 of DJF temperature reveals uniform spatial patterns over most of Pakistan, except extreme north, accounting for 84.38% of the total variance. The typical warm (cold) years were 1970, 1981, 1988, 1990, 1993, 2004, 2006, 2009, 2010 (1972, 1974, 1975, 1984, 2008, 2012). Favorable atmospheric conditions for warm temperature events (DJFTs) in Pakistan is an anomalous anticyclone spread over northeast Pakistan to Tibet at low to upper levels. This condition is controlled by the south and western part, of which there are significant southerly and convergent flows at low level with ascending motion over the study area. Further, examination revealed a close relationship of warm DJFTs with Western Indian Ocean warming and Eastern Indian Ocean indices but insignificant relation with the Nino3.4 index. Ocean warming related to Dipole Mode Index over eastern Indian Ocean (DMIE) is more influential ($r = 0.51$) than over the western Indian Ocean (DMIW) index ($r = 0.37$). The Ocean warming related to DMIE (EIOW), especially in Nov-Dec-Jan (NDJ) season, forced a significant ascending motion locally and then induced warm DJFTs-associated circulation pattern, propagating northward to Europe. By the dynamic diagnosis, the adiabatic and diabatic heating for the warm DJFTs is not remarkable. However, the horizontal temperature advection is positive and significant over most parts of Pakistan, both in the DJF and NDJ season, from the surface to the top of the troposphere. It suggests that the warm temperature advection is the possible prominent way of the EIOW on the warm DJFTs.

1. Introduction

The recent IPCC sixth assessment (AR6) report reported a rise in global mean surface temperature by 0.85 °C per decade between 1880 and 2020 on a regular scale (IPCC, 2021). The temperature variation is associated with extreme weather events in the form of droughts (Adnan et al., 2016; Ahmed et al., 2019; Ain et al., 2020), heatwaves (Khan et al., 2019a, b, c, 2020), flashfloods (Houze et al., 2011; Ahmad et al., 2016) and Glacial lake outburst floods (Tariq et al., 2014; Amin et al., 2020) have been reported over the region. Temperature and its extremes

Abbreviations: DMI, Dipole Mode Index; EIO, Eastern Indian Ocean Warming; DJFTs, DJF warm and cold events; DJF, December January February; EOF, Empirical Orthogonal Function.

* Corresponding author. Key Laboratory of Meteorological Disaster, Ministry of Education (KLME)/Joint International Research Laboratory of Climate and Environment Change (ILCEC), Nanjing, University of Information Science and Technology, Nanjing, 210044, China.
E-mail addresses: rizwan555danyore@gmail.com (R. Karim), tanguirong@nuist.edu.cn (G. Tan), bayugi@seoultech.ac.kr, ayugi.o@gmail.com (B. Ayugi), m_alriah@nuist.edu.cn (M.A. Ahmed Alriah), hamynads@gmail.com (H. Ngoma).

https://doi.org/10.1016/j.jastp.2022.105996
Received 14 September 2022; Received in revised form 8 December 2022; Accepted 9 December 2022
Available online 14 December 2022

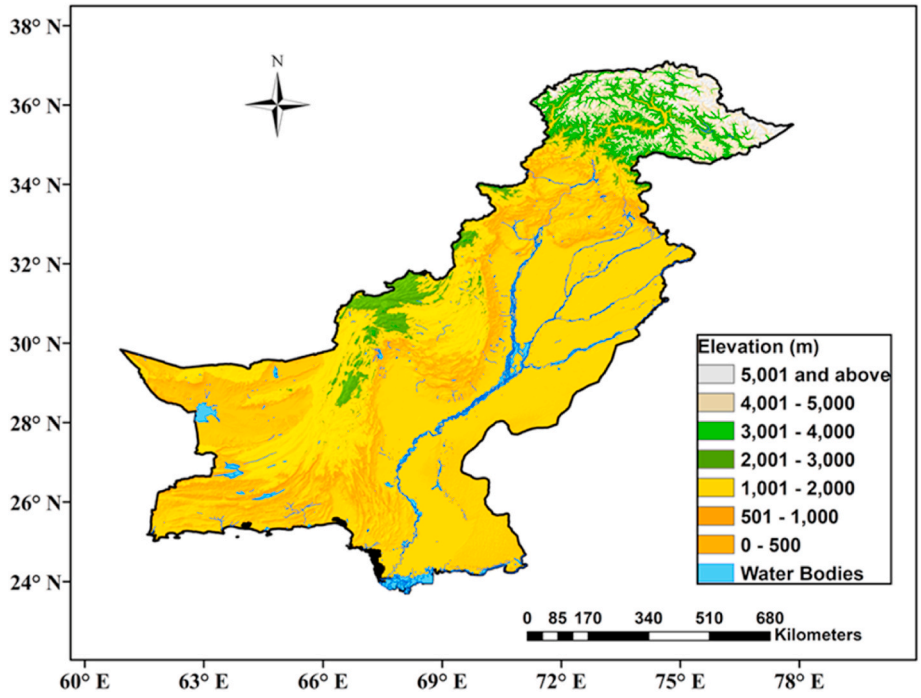

Fig. 1. Topography (m) map of the study area showing the latitudes and longitudes of Pakistan. The legend key on right side classifies the altitude (meters) of the study area.

have increased in the western part of South Asia, with a severe and frequent rise in the spatial extent of its impacts in recent years (Khan et al., 2019b).

Pakistan is among the top 10 (8th) most vulnerable countries to climate change (Eckstein et al., 2021). Various studies acknowledge temperature change implications on Pakistan's agriculture, hydrology, economy, environment, and public welfare (Khatoon and Ali, 2004; Rasul et al., 2012; Hussain et al., 2018). Studies by (McSweeney et al., 2012; Del Río et al., 2013; Adnan et al., 2017; Khan et al., 2019a) over Pakistan outlined higher warming rates during winter than in the summers, which may pose severe implications on water security of Pakistan. The winter season records the second most significant contribution to water supply; about 30% of the annual rainfall is accumulated in the form of glaciers and feeds water needs for the rest of the year (Hussain and Lee, 2013; Ali et al., 2015; Latif et al., 2017) across the country in sectors such as industries, agriculture, drinking, etc. (Ahmed et al., 2020).

Large-scale meteorological patterns, ranging from synoptic to planetary-scale structures, are associated with extreme temperature events (Davey et al., 2014; Del Río et al., 2013; Horton et al., 2015). The large-scale meteorological patterns are products of large displacements of air masses, creating large-amplitude wave patterns (Grotjahn et al., 2016). The synoptic conditions are induced by large-scale meteorological patterns, resulting in extreme events and may impact the teleconnection pattern (Cellitti et al., 2006). In some cases, the large-scale meteorological patterns are understood as juxtaposition (contrast) of teleconnection patterns that lead to extreme events (Konrad, 1996). Regional surface temperature changes lead to hypotheses linking these changes with large-scale circulations assumed under frequency, persistence, and duration of temperature (Horton et al., 2015).

Regional surface temperature is modulated by various teleconnection patterns, prominently the North Atlantic Oscillation (NAO), Arctic Oscillation (AO), and other associated atmospheric circulation patterns (Liu and Alexander, 2007; Del Río et al., 2013; Davey et al., 2014). The global interdecadal variations in Walker circulation (Hou et al., 2018), Asian-Pacific Oscillation (APO), and the Pacific Decadal Oscillation (PDO) (Yasunaka and Hanawa, 2006) are observed to be closely associated with global temperature modulation. Whereas the patterns of Pacific-North American pattern (PNA), Tropical-Northern Hemisphere pattern (TNH), North Pacific pattern (NP), Western Pacific pattern (WP), and circumglobal teleconnection (CGT) are known to have diverse roles (Chen and Song, 2019; Yu et al., 2019). Other systems like the Jet streams (Liang et al., 1996; Yang et al., 2002), and blocking high (Li et al., 2019) are also know to effect the variation of surface air temperature. These patterns or systems may influence the Siberian High (SH), Okhotsk high, which triggers temperature changes (Yasunaka and Hanawa, 2006; Li et al., 2013). However, the most important drivers of global/local temperature and associated circulation patterns are the tropical SSTs, including not only El Niño–Southern Oscillation but also decadal oscillations (Tan et al., 2017; Attada et al., 2018, 2019; Saleem et al., 2021) like the Atlantic Multidecadal Oscillation (AMO) and the North Pacific Oscillation (NPO) (Del Río et al., 2013).

Over Pakistan, the research in determining temperature variability associated with regional and global large-scale circulation variables are scarce. In one study, Del Río et al. (2013) detected higher correlations between temperatures over Pakistan and teleconnection patterns in the months of March-April-May. The NAO teleconnection was strongly associated with temperature modulation in the summer and spring seasons. Similarly (Saleem et al., 2021), reported a strong association of annual and seasonal changes (strongest in spring) in extreme temperature over Pakistan with La Nina (El Nino) events over the Pacific Ocean. The La Nina episodes have a more substantial influence on the intensity of highly high-temperature events over arid to semi-arid climatic zones.

Under the limited studies, a significant gap is left in understanding the role of circulations in temperature variation across temperature sensitive regions (Liu and Alexander, 2007; Saleem et al., 2021). Moreover, the long-term dominant temperature anomalies demand analysis of associated dynamic atmospheric parameters, i.e., Hadley cells, jet streams, storm tracks, and planetary waves (D'Agostino and Lionello, 2017). Consequently, this study has been designed to analyze the December 1969 to February 2014 temperature over Pakistan and the associated drivers. Our study deepens our understanding of the significant drivers of winter season temperature variability over Pakistan and associated mechanisms. The work has been outlined as: the Study area,

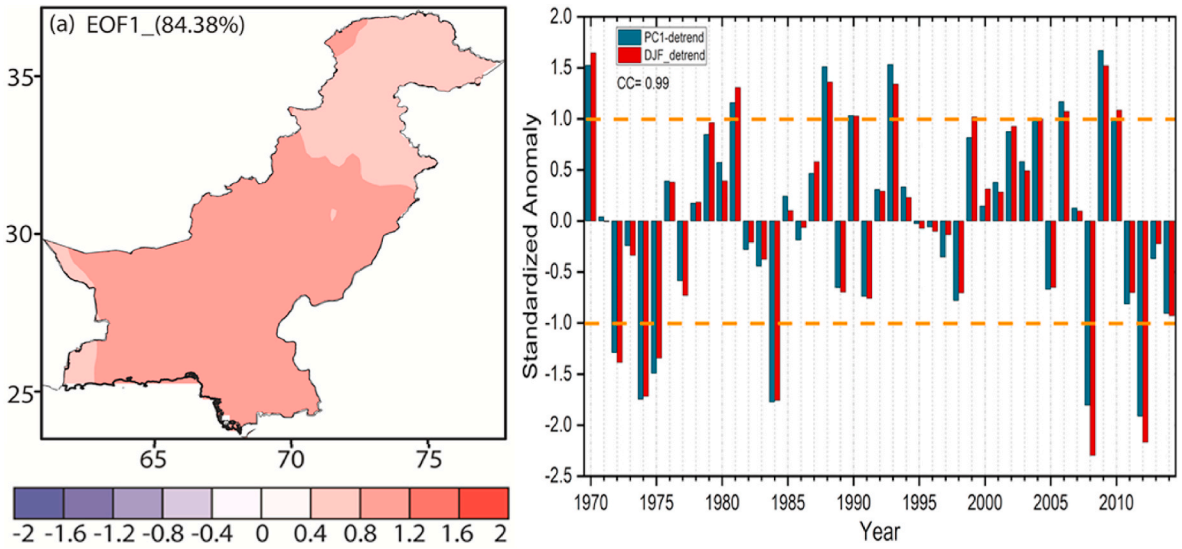

Fig. 2. The DJF dominant eigenvector (EOF1) distribution over Pakistan (a), its timeseries (PC1), and Inter–annual variability of DJF temperature over Pakistan for 1970–2014. The orange lines defines the dominant warm and cold years for PC1 and DJF temperature, respectively. The temperature timeseries is developed with detrended data.

datasets, and methods are mentioned in Section 2. The seasonal temperature results, circulation dynamics and teleconnections associated with warm/cold years, including the mechanisms of the most important drivers as the Indian Ocean's influence on the temperature are discussed in section 3. The conclusions of study are presented in Section 4.

2. Data and methods

2.1. Study area

Pakistan is located in the South Asian region between latitudes 23.5°N to 37.3°N and longitudes 61°E to 78°E, covering an area of 796,095 km2 (Asmat and Athar, 2017), as shown in Fig. 1. The south-north elevation gradients define the southern regions with lower elevations over Arabian Sea coastlines and the northern regions with higher elevations as the Himalayan and Karakorum Mountain ranges (Khan et al., 2019c). The spatial variability of temperature in the country is defined by the majority of regions' arid (southern regions) and semi-arid (central Punjab plains and north) climates, characterized by hot summers. Northern parts are characterized by a semi-arid to humid climate with cold winters and mild summers (Hussain and Lee, 2009; Khan et al., 2019b).

The diverse topography of Pakistan strongly influences the average temperature variability in Pakistan. Under the significant Spatio-temporal climate variability, the seasons' duration and onset vary over the country. The climate of the country is dominantly characterized by cold winters (December to February) and hot summers (May to August) due to diverse variations in temperature and precipitation (Asmat and Athar, 2017; Asmat et al., 2018; Khan et al., 2020). Spatially, temperature over northern regions ranges from −13 °C in winter (minimum) to 19.5 °C in summer (maximum). Over the southern half, minimum (winter) temperature of 0 °C–13 °C and maximum (summer) temperature of 25–35 °C is recorded (Ahmed et al., 2014; Khan et al., 2019b, 2019c). The intricate combination and functioning of hot monsoon spells in summer and western systems fed rainfalls in winters under land-sea temperature gradients and anomalies, and macro mechanisms in the complex geography mark the country's climate complex (Zahid and Rasul, 2011; Asmat et al., 2018).

2.2. Datasets and methods

2.2.1. Datasets

This study acquired the monthly surface air temperature gridded dataset of the Climate Research Unit (CRU) for 1970–2014 for DJF spatio-temporal analysis. The CRU dataset for temperature has been available over land points at a resolution of 0.5° × 0.5° since 1901 from quality-controlled data of 64,400 stations worldwide (Harris et al., 2014). The winter season was defined as the average of a variable for the months of December to February.

The troposphere can modulate surface temperature variability under the physical and dynamic processes such as subsidence and advection. To explain the dynamics behind temperature variability, large-scale circulation parameters at various vertical pressure levels in the DJF season during 1970–2014 were analyzed with composite and correlation analysis. Monthly mean circulation variables of zonal (u) and meridional (v) winds, mean sea level pressure, vertical velocity, atmospheric temperature at various vertical pressure levels of 2.5° × 2.5° horizontal resolution for 1970–2014 duration were obtained from the National Centers for Environmental Prediction–National Center for Atmospheric Research (NCEP–NCAR) from https://psl.noaa.gov/data/gridded/data.ncep.reanalysis.html. The velocity potential and stream function fields are also calculated from above data.

DJF months' Nino3.4 and Dipole Mode Indices (DMIE and DMIW) were also analyzed with Pearson linear correlation equation. The Nino 3.4 index is defined as the sea surface temperature (SST) anomalies between 170°W and 120°W and 5°S to 5°N over the western central Pacific and can be accessed at https://psl.noaa.gov/data/timeseries/monthly/NINO34/. The Dipole mode index features the anomalous SST gradient between the western equatorial Indian Ocean (50E-70E and 10S–10N) and the southeastern equatorial Indian Ocean (90E-110E and 10S–0N). The DMI is available at https://psl.noaa.gov/gcos_wgsp/Timeseries/DMI/.

2.2.2. Methods

The Empirical Orthogonal Function (EOF) technique following Lorenz (1956) was utilized over the standardized DJF temperature to determine its dominant modes of variability from 1970 to 2014. The variability in time series is accumulated into few major modes (Eigenvalues) and a time series (Principal Component) for each mode or eigenvectors is created as well. The dominant EOFs of the DJF surface air

Table 1
EOF 1 warm and cold years based on DJF mean temperature (°C) events over Pakistan for the 1970–2014 time period, where z represents standardized anomaly.

Season	Grades	Years	Anomaly (z)	Occurrence (%)
DJF	Warm Years	1970, 1981, 1988, 1990, 1993, 2004, 2006, 2009, 2010	$z \geq 1$	13.33
	Cold Years	1972, 1974, 1975, 1984, 2008, 2012	$z <= -1$	13.33
	Normal Years	1971, 1973, 1976, 1977, 1978, 1979, 1980, 1982, 1983, 1985, 1986, 1987, 1989, 1991, 1992, 1994, 1995, 1996, 1997, 1998, 1999, 2000, 2001, 2002, 2003, 2005, 2007, 2011, 2013, 2014	$-1 < z < 1$	73.33

temperature were used to identify hot and cold years for a composite analysis of associated circulation variables. The dominant PCs of the DJF surface air were used to choose hot and cold years for composite analysis of associated circulation variables. The warm and cold events/years are those whose normalized standard deviation is ≥ 1 and ≤ -1, respectively.

The Composite analysis technique identifies and averages the category/categories of common fields for variable/s selected according to their association with key conditions (Harou et al., 2006). The values at a grid point for a field on specified 'target' time are averaged together. The composite variables were also statistically tested for significance with the Student t-test.

To further diagnose the mechanisms for anomalous DJF surface air temperature events (DJFTs), the thermodynamic temperature equation is used to diagnose the role of different terms, which may be written as:

$$\frac{\partial T}{\partial t} = -\vec{v} \bullet \nabla T + S\omega + \frac{Q}{c_p} \quad (1)$$

where $\vec{v} = (u, v)$ is the horizontal wind velocity, ω is the p − vertical velocity, $S = \alpha/Cp - \partial T/\partial p$ denotes the atmospheric stability parameters, α is the specific volume of air, Cp is the specific heat of air and Q denotes the rate of diabatic heating, which is calculated following Yanai and Li (1994). Other symbols follow convention in meteorology.

3. Results and discussion

3.1. DJF surface air temperature variability

Fig. 2 shows the DJF dominant eigenvectors (EOF1) distribution over Pakistan, its associated timeseries PC1 and the interannual variability of DJF surface air temperature over Pakistan for 1970–2014. The temporal variability of the first three dominant modes explained 84.38%, 10.84%, and 04.78% (not shown), respectively, totaling 99.99% of the variance. The EOF1 (Fig. 2 a) extends exhibiting a uniform pattern over Pakistan, with strong loadings over the southern and weaker patches over the north and southwest corners. The PC1 (Fig. 2b) well captures the observed patterns of DJF temperature interannual variability with 24 (21) positive (negative) anomalies and is strongly (0.99%) correlated to the standardized DJF temperature for 1970–2014. The significant years (Table 1) of anomalous warm and cold temperature exceeding the threshold standardized anomaly of ≥1 (≤-1) are detected as: 1970, 1981, 1988, 1990, 1993, 2004, 2006, 2009, 2010 (1972, 1974, 1975, 1984, 2008, 2012) respectively. Following these years, further analyses assessed any association of winter warm and cold events (DJFTs) with

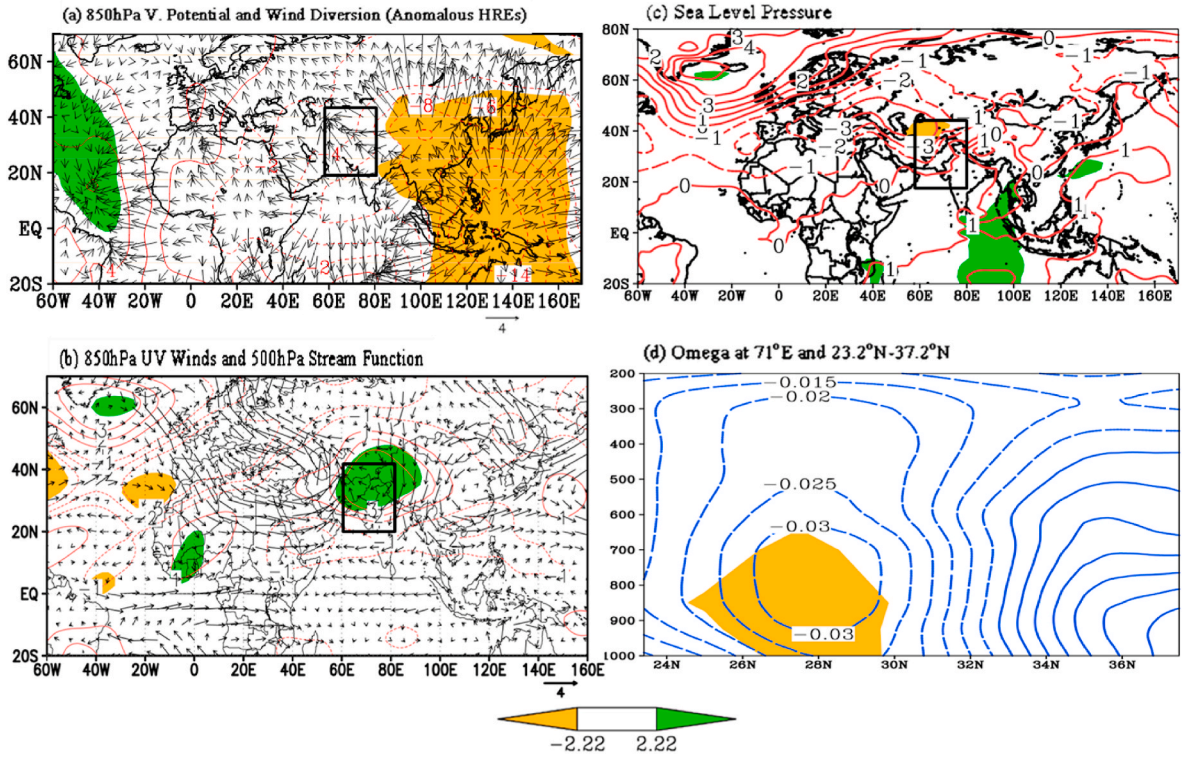

Fig. 3. Composites of differences for warm and cold years during 1970–2014 DJF season given for (a) 850 hPa meridional winds (m/s) and normalized velocity potential (m_2/s) given in contours, (b) normalized stream function (psi) at 500 hPa and 850 hPa UV winds (c) Sea Level Pressure (hPa), (d) Omega (Pa/s). Omega anomalies are outlined over Pakistan at fixed longitude [71°E] and latitudes of (23.2°N-37.2°N). Negative (dashed)/positive values indicate upward/downward motion. The shaded areas represent the values exceeding the 95% confidence level (Student t-test) based on the effective number of degrees of freedom for winds, velocity potential, SLP, Stream Function and Omega.

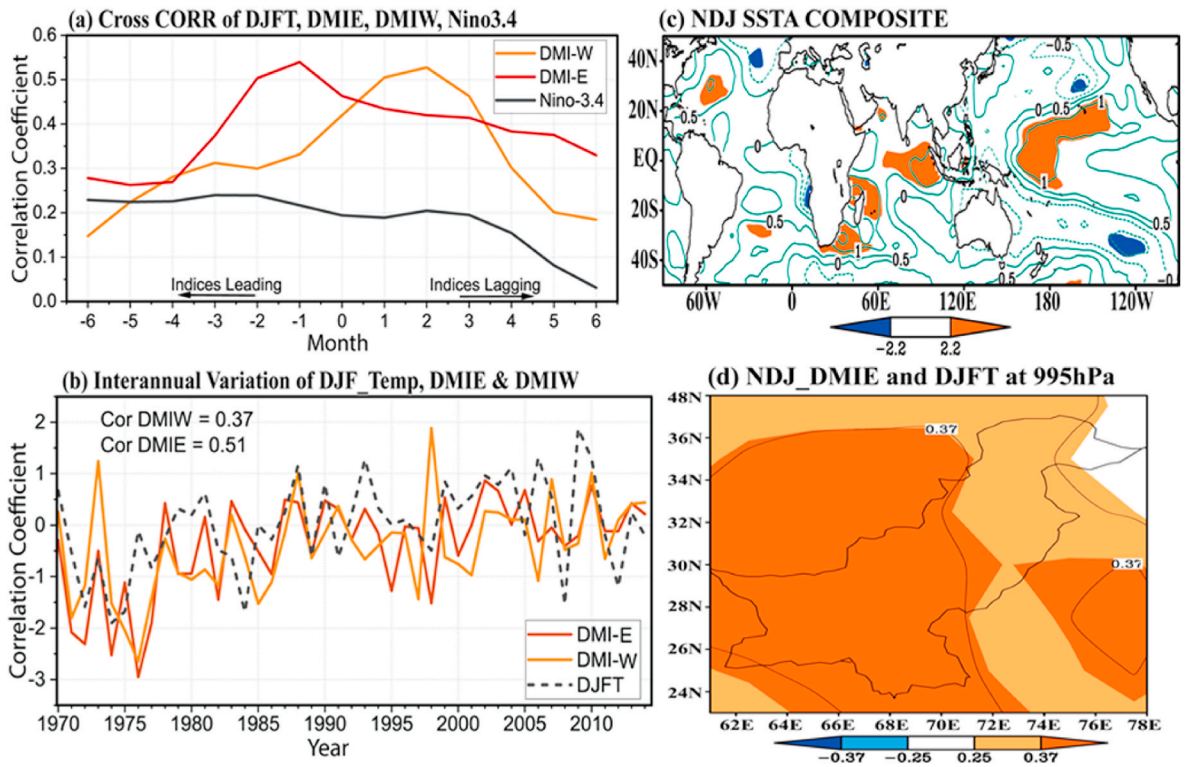

Fig. 4. The cross correlation (a) of DJF temperature (°C) over Pakistan with Equatorial Pacific Ocean ENSO index, Indian Ocean DMIW and DMIE index during Jan 1969 to Dec 2014; (b) the annual variation of DJF temperature (°C), DMIE and DMIW; (c) Composite SSTA differences for NDJ months' EIO events; (d) Correlation distribution between the temperature (°C) at 995 hPa and the NDJ (Nov–Jan) DMIE index. The shaded areas in (c) and (d) signify values exceeding 95% confidence level.

various influencing factors.

3.2. Circulation patterns of DJFTs

Fig. 3 shows composite differences for DJF months' warm and cold years during the 1970–2014. At 850 hPa (Fig. 3a), significant southerly winds from the adjacent Arabian Sea and Indian ocean cover most of the study region apart from the northeast, as the western part of a significant anticyclone is prevalent over the Northeast of Pakistan to Tibet area. The winds are convergent over the country, indicating warm advection from the south in warm years. At the upper level (500 hPa), there is also an anomalous anticyclone over the northeast and a cyclone to the south (Fig. 3b) extending to the eastern and western Indian Ocean, respectively, exhibiting a wave train. Studies have associated weakening (strengthening) of upper level Asian westerly jet (Yadav, 2016), anomalous easterlies (westerlies) over the subcontinent (Hunt et al., 2018) in warm (cold) events. Others observed a shifting of westerlies northward and replacement by persistent easterlies over Pakistan which blocked moisture supply from the Arabian Sea over the region during warm winters by reshaping the winds position, strength and flow (Ahmed et al., 2020; Khan et al., 2019c; Malik et al., 2012).

These studies are consistent with those shown in Fig. 3a, under the control of easterly flows in the south of the anticyclone over nnortheastern Pakistan in warm DJFTs. The sea level pressure is remarkably lower than normal when it is during warm DJFTs (Fig. 3c) over Pakistan. Similar conditions of south-easterlies from Arabian Sea and persistent lower sea level pressure conditions extending from Arabian Peninsula to Western India have been observed by Ahmed et al., (2020) and Attada et al. (2019). As a result, a prominent ascending motion is visible (Fig. 3d) over the latitudinal zone of 20°N to 32°N and is consistent with the typical warm years of lower than normal pressure (Fig. 3c) over the country with low cyclonic and southerly convergent flows at a low level. The upper-level anomalous anticyclone also seems prevailing during the occurrence of the ascending motion.

Primarily, the convergence of warm air with the ascent from surface to high levels during warm years causes higher surface temperature, which confirms the previous examination, that pressure troughs and the sharp rise in surface temperature over Pakistan and Afghanistan have been associated with the warm events (Khan et al., 2019c; Malik et al., 2012). However, what kind of land-sea-atmospheric dynamics are responsible for the above observed remarkable circulation anomalies? From Fig. 3a, the most prominent velocity potential anomalies are over the tropical western Pacific, besides the one located near the study area at 850 hPa level. The opposite anomalies delineated for 200hpa over the two areas (not shown) show positive (negative) velocity potential anomalies at low(upper) levels, denoting ascending motion. These results further support the analysis in the context that anomalous ascending motion appears during the warm years. In addition, significant anomalies in the tropical ocean denote stronger than normal boundary forcing in the area. The composite of global sea surface temperature anomalies for warm DJFTs revealed (not shown) significant warming over the Indian, Eastern Pacific, and Tropical Atlantic Oceans, which might be the leading cause of the warm DJFTs.

3.3. The related tropical drivers of DJFTs

To check the potential drivers of the DJFTs, the relationship between temperature and indices associated with ENSO and DMI was investigated. The association of DJFTs over Pakistan with the ENSO (Nino-3.4), DMIW, and DMIE indices are analyzed (Fig. 4) using linear correlation.

The correlation of surface temperature over Pakistan and the Nino3.4 index yield weak and insignificant positive correlations, while the correlation coefficients with the two DMI indices (Fig. 4a) are primarily significant ($r \geq 0.28$) at a confidence level of 0.05. However, the DMIE has the most significant leading correlation coefficient (0.54) with the DJF temperature, and the DMIW has the most significant lagging

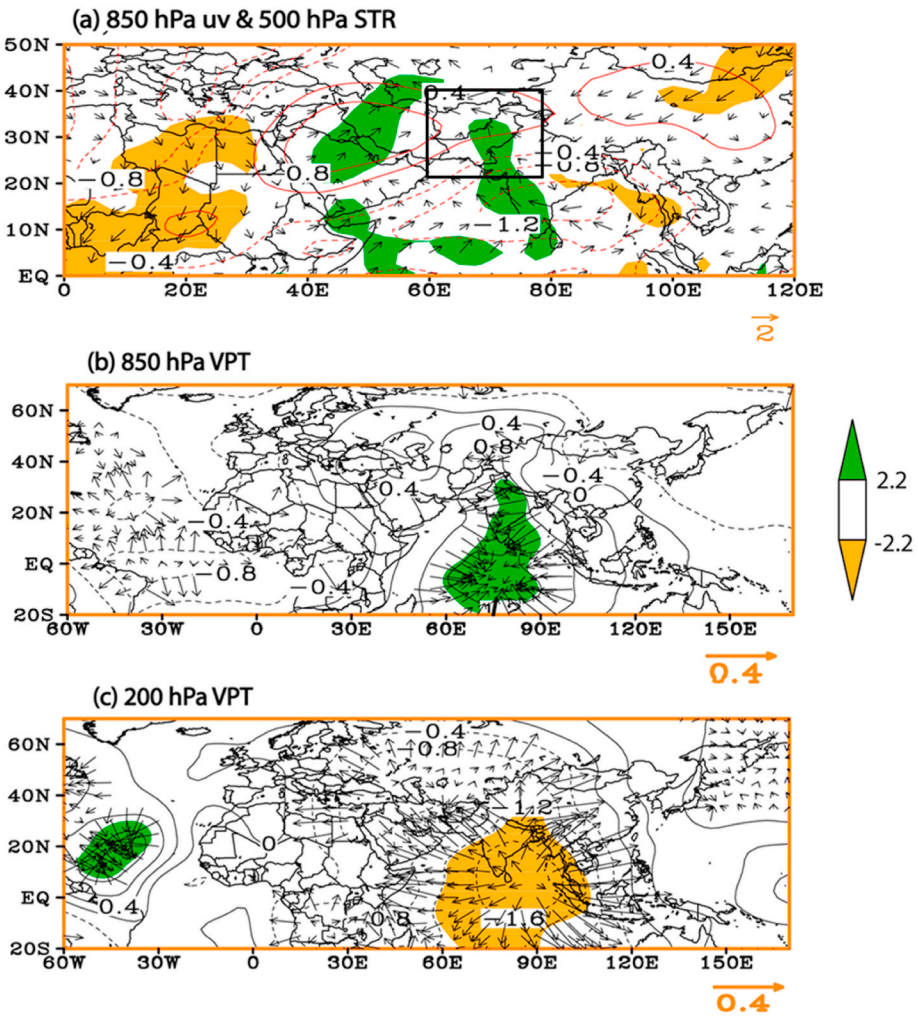

Fig. 5. Composite differences of normalized anomalies for warm and cold EIO during 1970–2014. (a) 850 hPa winds (m/s) and 500 hPa stream function (psi) of DJF; (b) 850 hPa velocity potential (850 hPa) of NDJ; (c) 200 hPa velocity potential (m^2/s) of NDJ with the insignificant fields omitted. The shaded areas represent values exceeding the 95% confidence level (Student t-test) based on the effective number of degrees of freedom, it is for the meridional wind in (a).

correlation (0.53). The association is stronger at the confidence level of 0.05 from the 3-month leading to 6-month lagging with the DMIE, but to the 4-month lagging with DMIW.

As the correlation coefficients of the two DMI indices with DJFTs are significant before (Nov–Jan months) the occurrence of DJFTs, it suggests that the anomalous ocean heating in the west and east may impact the DJFTs over Pakistan. However, since the DMIE has larger leading and contemporary correlation coefficients with the DJFTs (Fig. 4b), the ocean warming related to DMIE is more influential than that of the DMIW. The annual variations in the DJF surface air temperature, DMIE, and DMIW are shown in Fig. 4b. Correlations between DJF surface air temperature over Pakistan and DMIW index yield a significant positive correlation (0.37), however correlation between DJF surface air temperature and DMIE index is higher (0.51), following the cross correlations in Fig. 4a. The 6 years with most anomalous higher and lower DMIE exceeding the threshold standardized anomaly of ≥ 1 ($\leq$-1) are chosen as typical DMIE events i.e. 1987, 1999, 2002, 2003, 2005, 2010 (1971,1972, 1974, 1976, 1977,1998). The Indian Ocean interannual variability or Indian Ocean Dipole (IOD) is recognized to influence the Indian Ocean warm pool and exhibit diverse roles in the climate system (Webster et al., 1999).

From the composite of Sea Surface Temperature Anomalies (SSTA), differences for typical DMIE events (Fig. 4c), marked warm SSTAs over the Eastern Indian Ocean, and significant horseshoe shape warming in the mid-eastern tropical Pacific. According to the noticeable velocity potential anomalies seen over the western Pacific, the tropical Atlantic Ocean is warming (Fig. 3a). The spatial distribution of the correlation coefficients between NDJ (November, December, and January) DMIE and the DJF temperature at 995 hPa (Fig. 4d) are found significant over the whole country, with correlation coefficients larger than 0.372 at the confidence level of 0.01. The results suggest that the warming in the Eastern Indian Ocean (EIOW) has the closest relation to the warm DJFTs. A study by Du et al. (2013) observed associated a positive SSTA in winter with subsidence over the southeastern IO, followed by negative IOD during autumn, depicting the biennial nature of IOD with the longest known connection. Over South Asia, Chowdary et al. (2014) have similar observations with a weak association of El-Nino with surface temperature under low moisture transport while a positive correlation with Indian Ocean SST anomalies under negative sea level pressure and strong winds convergence. The EIOW is one of the important tropical drivers for the DJFTs. Therefore, the possible influential mechanisms of EIOW on the DJFTs were then investigated.

3.4. Possible mechanisms of DMI influence on DJFTs

From the analysis, the Indian Ocean, especially the eastern side warming related to DMIE, significantly influences temperature over the study domain. This suggests that the EIOW may have induced anomalous ascending motion over the warming area, which would have acted as tropical forcing. The wave-like circulation pattern could be induced

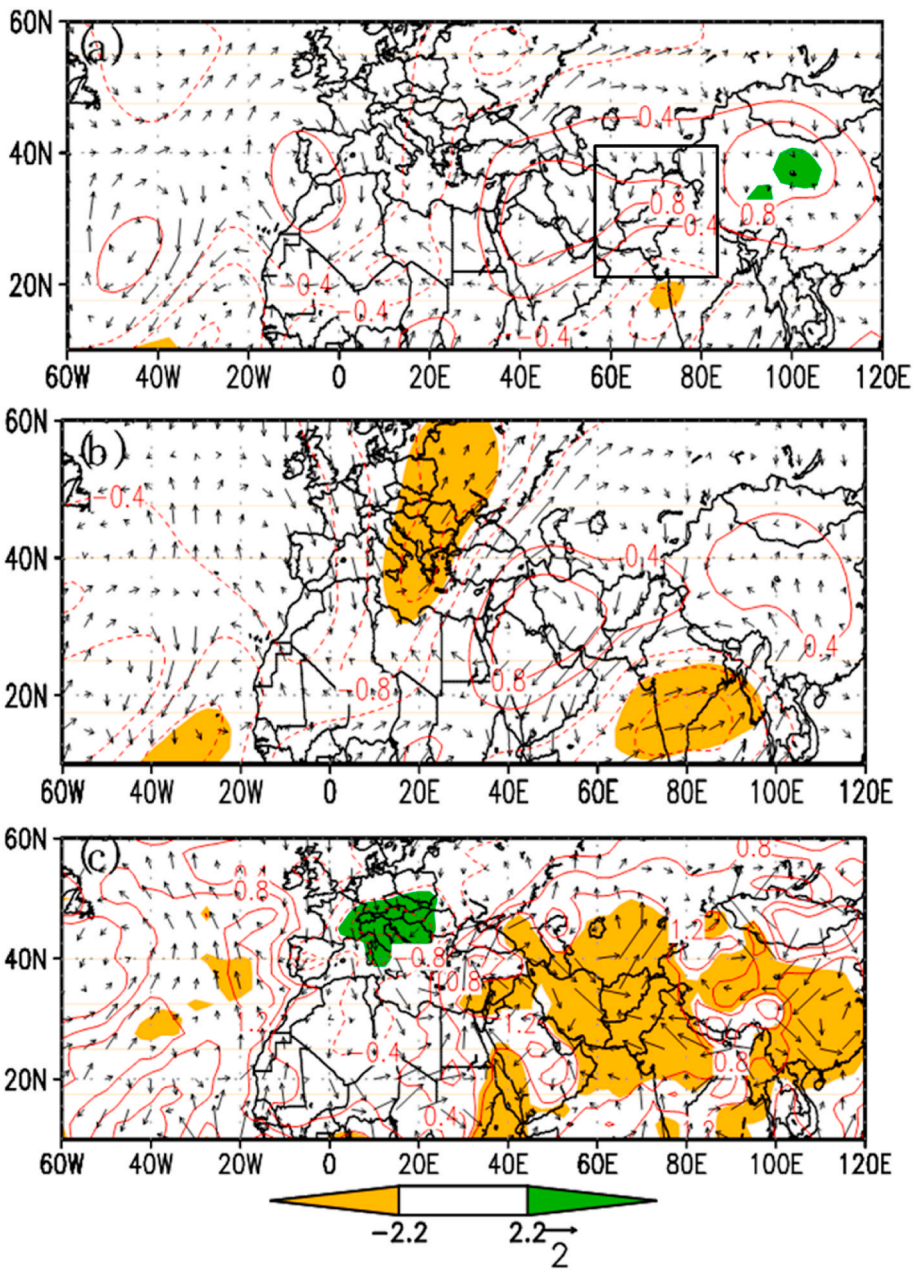

Fig. 6. Composite differences of the normalized anomalies of warm and cold events over EIO during 1970–2014. Composites of (a) 850 hPa winds (m/s) and 500 hPa stream function (psi) of NDJ; (b) 200 hPa winds (m/s) and 500 hPa stream function (psi) for NDJ months; (c) 995 hPa temperature (°C) and 850 hPa winds (m/s) in DJF months. Shaded areas represent values exceeding the 95% confidence level (Student t-test) based on the effective number of degrees of freedom, it is for the stream function in (a–b), but for the temperature in (c).

through such tropical forcing, like a Rossby wave response to tropical heating (Hoskins and Karoly, 1981; Tan et al., 2017). To detect the possible influence mechanisms of the EIOW on the DJFTs, the composite circulation anomalies for typical EIOW events are shown in Figs. 5 and 6. The most important feature of the warming conditions is the significant anticyclone over Tibet with significant southeasterly winds converging over Pakistan on the southern and western side of the anticyclone at 850 hPa in DJF (Fig. 5a). A wave train from EIO through Pakistan to Europe at 500hpa in the stream function fields is also observed, with a positive center in the middle near the Arabian Sea to Mediterranean areas and negative centers over EIO and southern Europe, respectively (Fig. 5a).

Furthermore, it is noted that Pakistan is under the influence of the positive center of wave train. The eastern portion of the train at 500 hPa and the anticyclone over Tibet at 850 hPa almost exactly match the circulation patterns associated with warm DJFTs as exhibited previously (Fig. 3b). The NDJ months' velocity potential composite at 850 hPa (Fig. 5b) show a significant positive anomalous center over the EIO extended westwards to Pakistan. A negative center visible at 200 hPa (Fig. 5c), denoting significant ascending motion over EIO is considered to be induced by the warming. This condition proposes that EIOW forces the significant circulation anomalies over the warming area. Further, significant descending motion is shown over the western Pacific for warm DJFTs at 500 hPa (Fig. 5b). This mass motion is not contradictory with the anomaly ascending over EIO (Fig. 5c). For this reason, the anomalous descending motion over the western Pacific could have been strengthened by the warming on both sides of the tropical ocean.

Then arguably, what kind of circulation pattern would have been induced by the EIOW forcing in NDJ? The composite differences between typical EIOW events in NDJ (Fig. 6a) provide a possible reason. A wave train pattern at 500 hPa from EIO through the Arabian Sea to the Eastern Mediterranean and southern Europe similar to the one during DJF (Fig. 5a) is clearly visible. However, the strengths of both negative centers over EIO and the Arabian Sea can be seen in the Mediterranean are weaker than those in DJF. At 850 hPa in NDJ, the southerly winds are visibly weaker than those in DJF over the EIO to Pakistan areas (Fig. 6a). It suggests that the EIOW in NDJ could be forcing the DJFTs-

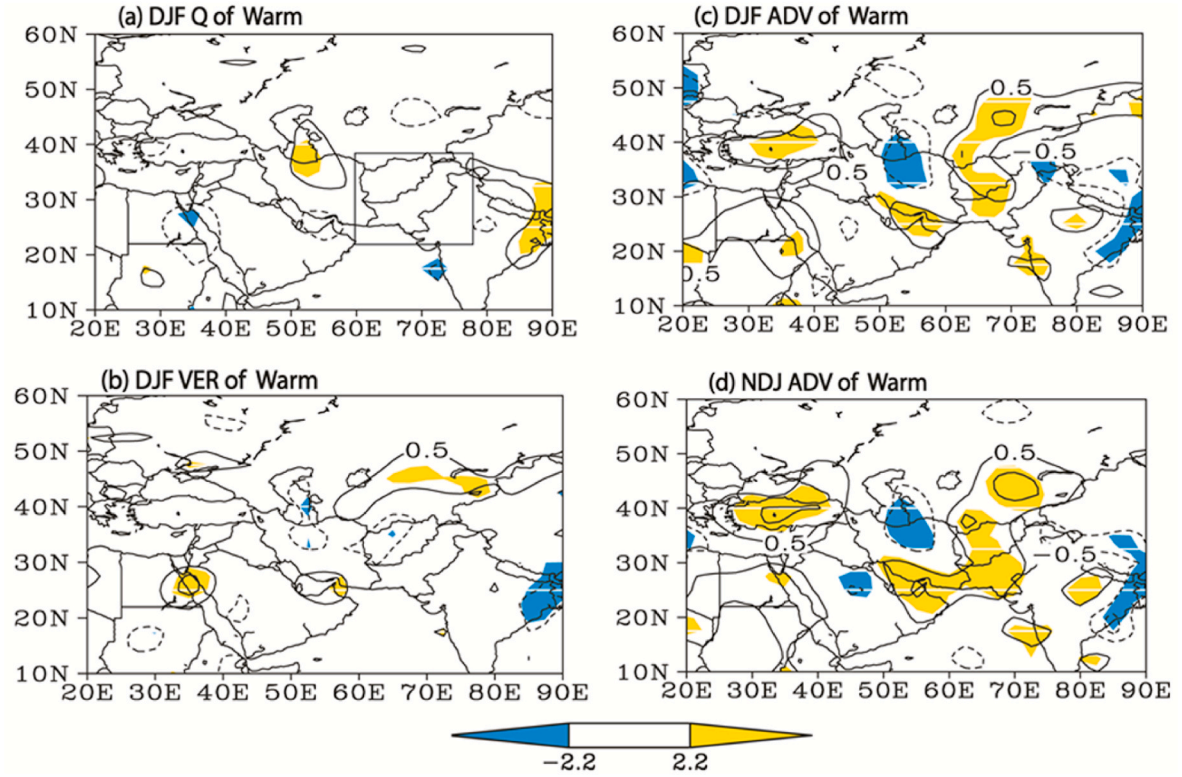

Fig. 7. Composite normalized anomalies for the typical warm DJFTs for (a) DJF adiabatic heating (W/m2); (b) DJF diabatic heating (W/m2); (c) DJF advection (oC/hour); and (d)NDJ advection (oC/hour) over box of 20o E to 90 o E longitudes and 10 o N to 60 o N latitudes. The shaded areas represent values exceeding the 95% confidence level (Student t-test) based on the effective number of degrees of freedom.

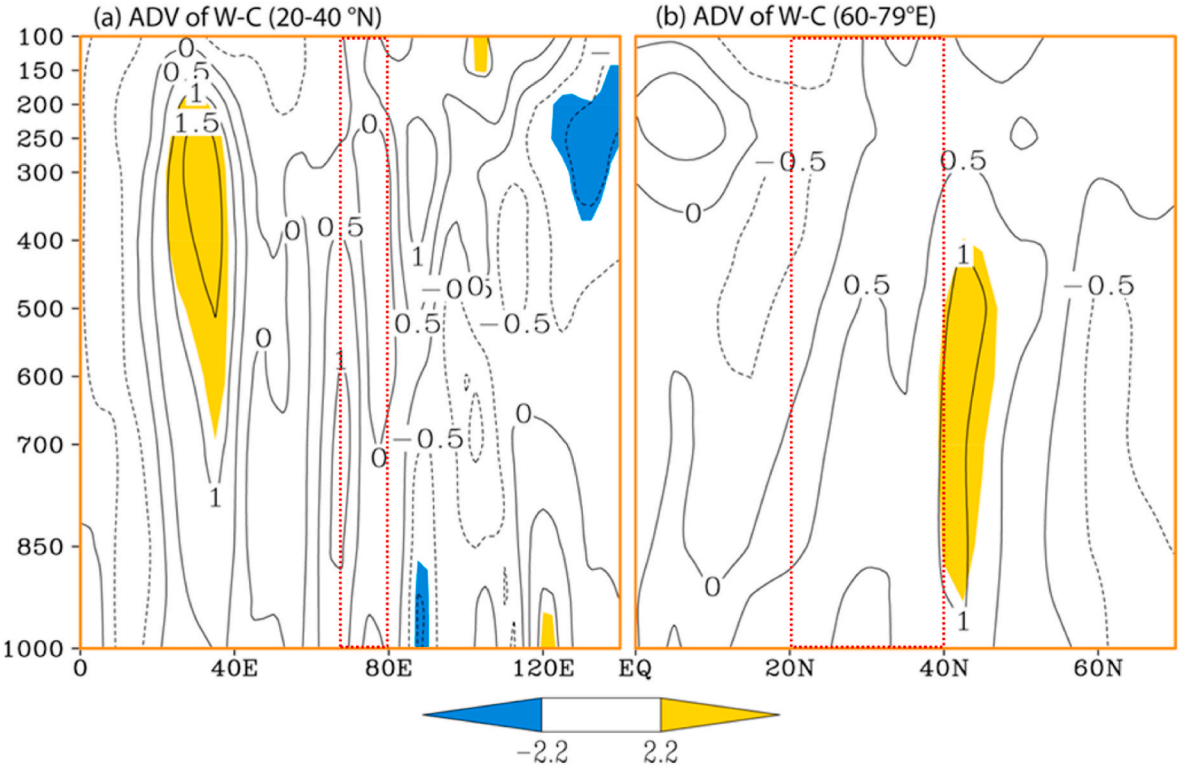

Fig. 8. The vertical-horizontal cross-sections of the composite temperature advection (^{o}C/hour) differences for DJFT events (a) averaged at latitudes of (20–40°N); (b) averaged at longitudes of (60–79°E). The shaded areas represent the values exceeding the 95% confidence level (Student t-test) based on the effective number of degrees of freedom.

associated circulation patterns and further patterns would propagate northward to Europe. In addition, the winds at 200 hPa (Fig. 6b) exhibit consistent circulation patterns with those at 500 hPa, and an anomalous anticyclone can be seen apparently over the Arabian Sea to the Eastern Mediterranean, corresponding to the anomaly positive center at 500 hPa. The anticyclone remains helpful in the detection of occurrence of the ascending motion. From Fig. 6c, the air temperature at 995 hPa is anomalously warm over the Indian Ocean spreaded to parts of the South Asian region, including Pakistan. The anomalous southerly flows induced by EIOW suggest warm air advection, which may have influenced the effect of EIOW on warm DJFTs.

The above analysis proposes that EIOW can induce DJFTs-associated circulation patterns influencing warm DJFTs. The warm temperature advection is the possible dominant way of the EIOW on the warm DJFTs. A dynamic diagnosis was carried out to confirm further the roles of the temperature advection on the DJFTs. The local temperature variation is determined by three terms temperature advection, diabatic heating, and adiabatic heating, which are shown on the right-hand side of temperature Equation (1).

The composite analysis of adiabatic, diabatic and advection heating are shown in Fig. 7. The composite anomalies for adiabatic (Fig. 7a) and diabatic (Fig. 7b) heating for the DJFTs reveal insignificant patterns at 850 hPa over Pakistan. Whereas, the horizontal temperature advection heating at 850 hPa in both DJF (Fig. 7c) and NDJ (Fig. 7d) is positive and significant over most parts of Pakistan. To further confirm whether the observed warm DJFTs occur due to advection, the vertical-horizontal cross sections composites of temperature advection are analyzed as shown in Fig. 8. A positive advection induced warming is visible at longitudinal (Fig. 8a) and latitudinal (Fig. 8b) sections. The positive and marked advection observed is not limited to low levels over the country since significant advection from the surface to the top of the troposphere is noticeable over the domains of 60–79°E longitude and 20–40°N latitude. This reveals that the advection heating caused the temperature rise during warm DJFTs.

4. Conclusions

Due to the high spatiotemporal variability of temperature in DJF across Pakistan and its hydrological, economic and environmental implications over the country, the leading modes of DJF temperature, related temperature (DJFTs) events, and associated mechanisms of the most important drivers affecting temperature variability of this season for 1970–2014 were examined.

The EOF1 of DJF temperature over Pakistan depicted a uniform variability pattern, accounting for 84.38% of the total variance. The typical warm (cold) years are 1988, 1993, 2004, 2006, 2009 and 2010 (1972, 1974, 1975, 1984, 2008 and 2012) during 1970–2014 period.

Favorable atmospheric conditions inducing the warm DJFT events in Pakistan were associated with an anomalous anticyclone over northeast Pakistan to Tibet from the low level to the upper level, under the control of the southern and western parts. This is characterized by significant southerly and convergent flows at a low level with ascending motion over the study area.

Further analysis revealed that DJFTs have a close association with the DMIE and DMIW indices but are insignificant to the Nino3.4 index. The Ocean warming related to DMIE is more impactful than that of DMIW in warm DJFTs. The DMIE related ocean warming (EIOW) forces significant ascending motion locally and then induces warm DJFTs-associated circulation patterns, propagating northwards to Europe.

The warm temperature advection is the possible inducing way of the EIOW on the DJFTs. From the dynamic diagnosis, both the adiabatic and diabatic heating for the warm DJFTs are not significant. The horizontal temperature advection delineated is positive and significant over most parts of the study region both in DJF and NDJ season, from the surface to the top of the troposphere. The advection induced heating caused the temperature rise during warm DJFTs.

This study only examined the possible relationship between the tropical Ocean in the leading time through the DJFTs-associated circulation pattern. It is noticeable that the composite significant velocity potential and SST anomalies over the western Pacific and tropical Atlantic Ocean (Fig. 3c) are also significant, while the EIOW is the primary driver for warm DJFTs in Pakistan. Mainly the annual variation of DJFTs is studied in this work. Chowdary et al. (2014) observed that though El-Nino peaks during winters, it has less impact on the temperature of the Indian subcontinent, which is consistent with the results of our work. Also, Du et al. (2013) stated that IO-SST anomalies impact on winter surface temperature is observable through modulation of IOD events based on wind changes which are in turn related to weakening/strengthening of Walker circulation in the Indian Ocean section in winter, which is in part forced through the fast Indian Ocean warming.

Significant components of the large-scale circulations (Hadley cell, jet streams, storm tracks, planetary waves) have changed in recent decades under climate change (Molnos et al., 2017), and therefore need in-depth studies. Future studies focusing on the mechanism and most important drivers for the future temperature change or what pathway would it be through on the DJFTs in Pakistan may be focused on in upcoming works. Further study under numerical models is also necessary.

Authors contribution

RK: Rizwan Karim, TG:Tan Guirong, BA: Brian Ayugi, AMAA: Alriah Mohamed Abdallah Ahmed, HN: Hamida Ngoma.

All authors made contribution to the development of manuscript. RK is the main author and TG is the coauthor and corresponding author of this work. The contributions from author and coauthors are: RK, TG, BA: conceptualization, formal writing, and original draft preparation. RK, TG, BA, MAAA, HN: Data curation, methodology, visualization. TG, RK, HN, BA: writing-review and editing, investigation. RK, BA, MAAA, TG: Validation, writing-review, and editing. TG: Funding acquisition, Editing, Supervision.

Funding statement

This research is conducted independently without any funding received or allocated by anyone.

Compliance with ethical standards

This work follows all the ethical standards in data collection, curation, and presentation under provided guidelines by the Nanjing University of Information Science and Technology.

Declaration of competing interest

The authors declare that they have no known competing financial interests or personal relationships that could have appeared to influence the work reported in this paper.

Data availability

Data will be made available on request.

Acknowledgments

The authors are thankful to the Nanjing University of Information Science and Technology for providing research encouraging environment. High gratitude towards the data centers, University of East Angelia (CRU), NOAA, and NCEP/NCEP for providing the datasets employed in the study.

References

Adnan, S., Ullah, K., Shouting, G., 2016. Investigations into precipitation and drought climatologies in south central Asia with special focus on Pakistan over the period 1951-2010. J. Clim. 29, 6019–6035. https://doi.org/10.1175/JCLI-D-15-0735.1.

Adnan, S., Ullah, K., Gao, S., Khosa, A.H., Wang, Z., 2017. Shifting of agro-climatic zones, their drought vulnerability, and precipitation and temperature trends in Pakistan. Int. J. Climatol. 37, 529–543. https://doi.org/10.1002/joc.5019.

Ahmad, B., Rana, A.S., Abuzar, K., Kiran, R., Mansoor, R., Kubra, S., 2016. Diagnostic study of heavy downpour in 2015 flash floods over chitral area, northern Pakistan. Pakistan J. Meteorol. 12, 79–93.

Ahmed, K., Shahid, S., Harun, S. Bin, 2014. Spatial interpolation of climatic variables in a predominantly arid region with complex topography. Environ. Syst. Decis. 34, 555–563. https://doi.org/10.1007/s10669-014-9519-0.

Ahmed, K., Shahid, S., Wang, X., Nawaz, N., Khan, N., 2019. Spatiotemporal changes in aridity of Pakistan during 1901-2016. Hydrol. Earth Syst. Sci. 23, 3081–3096. https://doi.org/10.5194/hess-23-3081-2019.

Ahmed, F., Adnan, S., Latif, M., 2020. Impact of jet stream and associated mechanisms on winter precipitation in Pakistan. Meteorol. Atmos. Phys. 132, 225–238. https://doi.org/10.1007/s00703-019-00683-8.

Ain, N.U., Latif, M., Ullah, K., Adnan, S., Ahmed, R., Umar, M., Azam, M., 2020. Investigation of seasonal droughts and related large-scale atmospheric dynamics over the Potwar Plateau of Pakistan. Theor. Appl. Climatol. 140, 69–89. https://doi.org/10.1007/s00704-019-03064-8.

Ali, S., Li, D., Congbin, F., Khan, F., 2015. Twenty first century climatic and hydrological changes over Upper Indus Basin of Himalayan region of Pakistan. Environ. Res. Lett. 10 https://doi.org/10.1088/1748-9326/10/1/014007.

Amin, M., Bano, D., Hassan, S.S., Goheer, M.A., Khan, A.A., Khan, M.R., Hina, S.M., 2020. Mapping and monitoring of glacier lake outburst floods using geospatial modelling approach for Darkut valley, Pakistan. Meteorol. Appl. 27 https://doi.org/10.1002/met.1877.

Asmat, U., Athar, H., 2017. Run-based multi-model interannual variability assessment of precipitation and temperature over Pakistan using two IPCC AR4-based AOGCMs. Theor. Appl. Climatol. 127, 1–16. https://doi.org/10.1007/s00704-015-1616-6.

Asmat, U., Athar, H., Nabeel, A., Latif, M., 2018. An AOGCM based assessment of interseasonal variability in Pakistan. Clim. Dynam. 50, 349–373. https://doi.org/10.1007/s00382-017-3614-0.

Attada, R., Yadav, R.K., Kunchala, R.K., Dasari, H.P., Knio, O., Hoteit, I., 2018. Prominent mode of summer surface air temperature variability and associated circulation anomalies over the Arabian Peninsula. Atmos. Sci. Lett. 19 https://doi.org/10.1002/asl.860.

Attada, R., Dasari, H.P., Chowdary, J.S., Yadav, R.K., Knio, O., Hoteit, I., 2019. Surface air temperature variability over the Arabian Peninsula and its links to circulation patterns. Int. J. Climatol. 39 (1), 445–464. https://doi.org/10.1002/joc.5821.

Cellitti, M.P., Walsh, J.E., Rauber, R.M., Portis, D.H., 2006. Extreme cold air outbreaks over the United States, the polar vortex, and the large-scale circulation. J. Geophys. Res. Atmos. 111 https://doi.org/10.1029/2005JD006273.

Chen, S., Song, L., 2019. Recent strengthened impact of the winter Arctic Oscillation on the Southeast Asian surface air temperature variation. Atmosphere 10. https://doi.org/10.3390/atmos10040164.

Chowdary, J.S., John, N., Gnanaseelan, C., 2014. Interannual variability of surface air-temperature over India: impact of ENSO and Indian Ocean Sea surface temperature. Int. J. Climatol. 34, 416–429. https://doi.org/10.1002/joc.3695.

Davey, M.K., Brookshaw, A., Ineson, S., 2014. The probability of the impact of ENSO on precipitation and near-surface temperature. Clim. Risk Manag. 1, 5–24. https://doi.org/10.1016/j.crm.2013.12.002.

Del Río, S., Anjum Iqbal, M., Cano-Ortiz, A., Herrero, L., Hassan, A., Penas, A., 2013. Recent mean temperature trends in Pakistan and links with teleconnection patterns. Int. J. Climatol. 33, 277–290. https://doi.org/10.1002/joc.3423.

Du, Y., Cai, W., Wu, Y., 2013. A new type of the indian ocean dipole since the mid-1970s. J. Clim. 26, 959–972. https://doi.org/10.1175/JCLI-D-12-00047.1.

D'Agostino, R., Lionello, P., 2017. Evidence of global warming impact on the evolution of the Hadley Circulation in ECMWF centennial reanalyses. Clim. Dynam. 48, 3047–3060. https://doi.org/10.1007/s00382-016-3250-0.

Eckstein, D., Künzel, V., Schäfer, L., 2021. Global Climate Risk Index 2021: Who Suffers Most from Extreme Weather Events? Weather-Related Loss Events in 2019 and 2000-2019. Ger. e.vol. 28.

Grotjahn, R., Black, R., Leung, R., Wehner, M.F., Barlow, M., Bosilovich, M., Gershunov, A., Gutowski, W.J., Gyakum, J.R., Katz, R.W., Lee, Y.Y., Lim, Y.K., Prabhat, 2016. North American extreme temperature events and related large scale meteorological patterns: a review of statistical methods, dynamics, modeling, and trends. Clim. Dynam. 46, 1151–1184. https://doi.org/10.1007/s00382-015-2638-6.

Harou, A.P., Lajoie, R.F., Kniveton, D.R., Frogley, M.R., 2006. The influence of the Indian Ocean dipole mode on precipitation over the Seychelles. Int. J. Climatol. 26, 45–54. https://doi.org/10.1002/joc.1239.

Harris, I., Jones, P.D., Osborn, T.J., Lister, D.H., 2014. Updated high-resolution grids of monthly climatic observations - the CRU TS3.10 Dataset. Int. J. Climatol. 34, 623–642. https://doi.org/10.1002/joc.3711.

Horton, D.E., Johnson, N.C., Singh, D., Swain, D.L., Rajaratnam, B., Diffenbaugh, N.S., 2015. Contribution of changes in atmospheric circulation patterns to extreme temperature trends. Nature 522, 465–469. https://doi.org/10.1038/nature14550.

Hoskins, B.J., Karoly, D.J., 1981. The steady linear response of a spherical atmosphere to thermal and orographic forcing. J. Atmos. Sci. 38, 1179–1196. https://doi.org/10.1175/1520-0469(1981)038<1179:TSLROA>2.0.CO, 2.

Hou, X., Cheng, J., Hu, S., Feng, G., 2018. Interdecadal variations in thewalker circulation and its connection to inhomogeneous air temperature changes from 1961-2012. Atmosphere 9. https://doi.org/10.3390/atmos9120469.

Houze, R.A., Rasmussen, K.L., Medina, S., Brodzik, S.R., Romatschke, U., 2011. Anomalous atmospheric events leading to the summer 2010 floods in Pakistan. Bull. Am. Meteorol. Soc. 92, 291–298. https://doi.org/10.1175/2010BAMS3173.1.

Hunt, K.M.R., Turner, A.G., Shaffrey, L.C., 2018. The evolution, seasonality and impacts of western disturbances. Q. J. R. Meteorol. Soc. 144, 278–290. https://doi.org/10.1002/qj.3200.

Hussain, M.S., Lee, S., 2009. A classification of rainfall regions in Pakistan. J. Korean Geogr. Soc. 44, 605–623.

Hussain, M.S., Lee, S., 2013. The regional and the seasonal variability of extreme precipitation trends in Pakistan. Asia-Pacific J. Atmos. Sci. 49, 421–441. https://doi.org/10.1007/s13143-013-0039-5.

Hussain, M., Liu, G., Yousaf, B., Ahmed, R., Uzma, F., Ali, M.U., Ullah, H., Butt, A.R., 2018. Regional and sectoral assessment on climate-change in Pakistan: social norms and indigenous perceptions on climate-change adaptation and mitigation in relation to global context. J. Clean. Prod. https://doi.org/10.1016/j.jclepro.2018.07.272.

Khan, N., Shahid, S., Ismail, T. bin, Wang, X.J., 2019a. Spatial distribution of unidirectional trends in temperature and temperature extremes in Pakistan. Theor. Appl. Climatol. 136, 899–913. https://doi.org/10.1007/s00704-018-2520-7.

Khan, N., Shahid, S., Ismail, T., Ahmed, K., Nawaz, N., 2019b. Trends in heat wave related indices in Pakistan. Stoch. Environ. Res. Risk Assess. 33, 287–302. https://doi.org/10.1007/s00477-018-1605-2.

Khan, N., Shahid, S., Juneng, L., Ahmed, K., Ismail, T., Nawaz, N., 2019c. Prediction of heat waves in Pakistan using quantile regression forests. Atmos. Res. 221, 1–11. https://doi.org/10.1016/j.atmosres.2019.01.024.

Khan, N., Shahid, S., Ahmed, K., Wang, X., Ali, R., Ismail, T., Nawaz, N., 2020. Selection of GCMs for the projection of spatial distribution of heat waves in Pakistan. Atmos. Res. 233, 104688 https://doi.org/10.1016/j.atmosres.2019.104688.

Khatoon, S., Ali, Q.M., 2004. Biodiversity of the semi-arid and arid regions of Pakistan: status, threats, and conservation measures. Ann. Arid Zone 43, 277–291.

Konrad, C.E., 1996. Relationships between the intensity of cold-air outbreaks and the evolution of synoptic and planetary-scale features over North America. Mon. Weather Rev. 124, 1067–1083. https://doi.org/10.1175/1520-0493(1996)124<1067:RBTIOC>2.0.CO, 2.

Latif, M., Syed, F.S., Hannachi, A., 2017. Rainfall trends in the South Asian summer monsoon and its related large-scale dynamics with focus over Pakistan. Clim. Dynam. 48, 3565–3581. https://doi.org/10.1007/s00382-016-3284-3.

Li, Q., Liu, Y., Song, H., Cai, Q., Yang, Y., 2013. Long-term variation of temperature over North China and its links with large-scale atmospheric circulation. Quat. Int. 283, 11–20. https://doi.org/10.1016/j.quaint.2012.03.017.

Li, M., Yao, Y., Luo, D., Zhong, L., 2019. The linkage of the large-scale circulation pattern to a long-lived heatwave over Mideastern China in 2018. Atmosphere 10. https://doi.org/10.3390/ATMOS10020089.

Liang, X.Z., Wang, W.C., Dudek, M.P., 1996. Northern hemispheric interannual teleconnection patterns and their changes due to the greenhouse effect. J. Clim. 2. https://doi.org/10.1175/1520-0442(1996)009<0465:NHITPA>2.0.CO.

Liu, Z., Alexander, M., 2007. Atmospheric bridge, oceanic tunnel, and global climatic teleconnections. Rev. Geophys. 45, 1–34. https://doi.org/10.1029/2005RG000172.

Lorenz, E.N., 1956. Empirical Orthogonal Functions and Statistical Weather Prediction. Technical report Statistical Forecast Project Report 1 Department of Meteorology MIT 49.

Malik, K.M., Mahmood, A., Kazmi, D.H., Khan, J.M., 2012. Impact of climate change on agriculture during winter season over Pakistan. Agric. Sci. 3, 1007–1018. https://doi.org/10.4236/as.2012.38122.

McSweeney, C., New, M., Lizcano, G., 2012. Climate change country profiles: Belize. Natl. Commun. Support Program. 67, 1–27.

Molnos, S., Petri, S., Lehmann, J., Peukert, E., Coumou, D., 2017. The sensitivity of the large-scale atmosphere circulation to changes in surface temperature gradients in the Northern Hemisphere. Earth Syst. Dyn. Discuss. 1–17. https://doi.org/10.5194/esd-2017-65.

Rasul, G., Afzal, M., Zahid, M., Ali Bukhari, S.A., 2012. Climate Change in Pakistan Focused on Sindh Province. https://doi.org/10.13140/2.1.2170.6560. Pakistan Meteorological Department Technical Report No. PMD-25/2012, Pakistan Meteorological Department Technical Report No. PMD 25/2012.

Saleem, F., Zeng, X., Hina, S., Omer, A., 2021. Regional changes in extreme temperature records over Pakistan and their relation to Pacific variability. Atmos. Res. 250 https://doi.org/10.1016/j.atmosres.2020.105407.

Tan, G., Ren, H.L., Chen, H., You, Q., 2017. Detecting primary precursors of January surface air temperature anomalies in China. J. Meteorol. Res. https://doi.org/10.1007/s13351-017-7013-6.

Tariq, S., Mahmood, A., Rasul, G., 2014. Temperature and precipitation : GLOF triggering indicators in gilgit-baltistan , Pakistan. Pakistan J. Meteorol. 10, 39–56.

Webster, P.J., Moore, A.M., Loschnigg, J.P., Leben, R.R., 1999. Coupled ocean-atmosphere dynamics in the Indian Ocean during 1997-98. Nature 401, 356–360. https://doi.org/10.1038/43848.

Yadav, R.K., 2016. On the relationship between Iran surface temperature and northwest India summer monsoon rainfall. Int. J. Climatol. 36, 4425–4438. https://doi.org/10.1002/joc.4648.

Yanai, Michio, Li, Chengfeng, 1994. Mechanism of heating and the boundary layer over the Tibetan Plateau. Mon. Weather Rev. 122, 305–323. https://doi.org/10.1175/1520-0493(1994)122<0305:mohatb>2.0.co.

Yang, S., Lau, K.M., Kim, K.M., 2002. Variations of the East Asian jet stream and Asian-Pacific-American winter climate anomalies. J. Clim. 15, 306–325. https://doi.org/10.1175/1520-0442(2002)015<0306:voteaj>2.0.co.

Yasunaka, S., Hanawa, K., 2006. Interannual summer temperature variations over Japan and their relation to large-scale atmospheric circulation field. J. Meteorol. Soc. Japan 84, 641–652. https://doi.org/10.2151/jmsj.84.641.

Yu, B., Lin, H., Soulard, N., 2019. A comparison of North American surface temperature and temperature extreme anomalies in association with various atmospheric teleconnection patterns. Atmosphere 10. https://doi.org/10.3390/atmos10040172.

Zahid, M., Rasul, G., 2011. Frequency of extreme temperature & precipitation events in Pakistan 1965-2009. Sci. Int. 23, 313–319.

IPCC, 2021: *Climate Change 2021: The Physical Science Basis. Contribution of Working Group I to the Sixth Assessment Report of the Intergovernmental Panel on Climate Change* [Masson-Delmotte, V., P. Zhai, A. Pirani, S.L. Connors, C. Péan, S. Berger, N. Caud, Y. Chen, L. Goldfarb, M.I. Gomis, M. Huang, K. Leitzell, E. Lonnoy, J.B.R. Matthews, T. K. Maycock, T. Waterfield, O. Yelekçi, R. Yu, and B. Zhou (eds.)]. Cambridge University Press, Cambridge, United Kingdom and New York, NY, USA, In press, doi: 10.1017/9781009157896.